This is a repository copy of *Instantaneous Power Control for Suppressing the Second Harmonic DC Bus Voltage under Generic Unbalanced Operating Conditions*.

White Rose Research Online URL for this paper:
http://eprints.whiterose.ac.uk/107210/

Version: Accepted Version

Instantaneous Power Control for Suppressing the Second Harmonic DC Bus Voltage under Generic Unbalanced Operating Conditions

Yashan Hu, Zi Qiang Zhu, *Fellow, IEEE,* and Milijana Odavic

[1] *Abstract*— **This paper proposes an simplified instantaneous output power control to suppress the second harmonic DC bus voltage due to asymmetry in a three-phase PWM converter system without any sequential component decomposers. Normally, in the instantaneous output power control, the positive and negative output voltages and currents are required and they are usually decomposed by notch filters or dual second-order generalized integrals that are difficult to tune and complicated. While in the proposed method, the positive-sequence and negative-sequence currents are regulated by PI plus resonant (PI-R) controllers in *dq*-frame. Therefore, the sequential current decomposers can be avoided. Meanwhile, the positive and negative sequence output voltages, which are essential for calculating the positive-sequence and negative-sequence current references, are simply obtained from the outputs of the PI and resonant controllers, respectively. The proposed method is robust to any asymmetries and its effectiveness is verified on a prototype asymmetric three-phase permanent magnet synchronous generator (PMSG) system with inherent and externally added asymmetries.**

Index Terms—**DC voltage pulsation, instantaneous power control, PWM rectifier, three-phase system asymmetry, unbalance.**

I. INTRODUCTION

IN practical three phase AC systems, unbalanced conditions are usually caused by small differences in the line impedances or voltage sources. They result in undesirable second harmonic (2h) DC bus voltage and 2h current flowing through the DC bus electrolytic capacitor [1-4], which is connected to the three-phase AC system through an interface PWM converter. Since the equivalent series resistance of an electrolytic capacitor increases at low frequencies, the 2h current will cause significant increase in power losses and temperature, which results in the capacitor's lifetime reduction [5].

The effective way to suppress the 2h DC bus voltage is to suppress the 2h power flowing through the DC bus capacitor by means of the instantaneous power control [4, 6-12] as they are closely related [13, 14]. In these power control methods, the negative-(*N*-) sequence currents were introduced to eliminate the 2h power in the DC bus. This approach has been widely employed in PWM rectifier systems in weak grids [4, 6-12] where the line voltages are usually unbalanced.

[1] The authors are all with the Department of Electronic and Electrical Engineering, The University of Sheffield, Sheffield, S1 3JD, U.K. (e-mail: yashan.hu@sheffield.ac.uk; z.q.zhu@sheffield.ac.uk; m.odavic@sheffield.ac.uk).
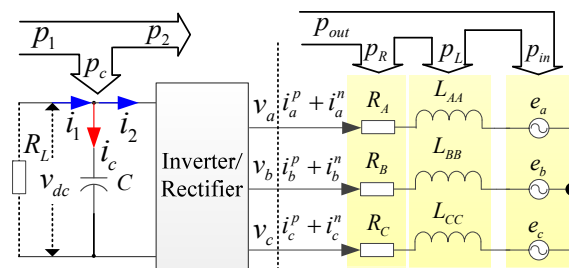

Fig.1 Conventional three phase PWM inverter/rectifier AC system.

To ease the review of the instantaneous power control methods, the block diagram of a PWM inverter/rectifier three phase AC system is shown in Fig.1, where e_a, e_b, and e_c denote the line voltages when the converter is connected to the grid or equivalently they denote 3-phase back electromotive forces (EMFs) in machine drive systems. The power generated by e_a, e_b, and e_c is denoted by p_{in}, while the power of the line impedance is denoted by p_R and p_L. The sum of p_{in}, p_R and p_L is defined as the total power p_{out}. Generally, three main types of the instantaneous power control were reported in literature.

The first method [6] is based on the instantaneous input power control, where the 2h power in p_{in}, the average power in p_{in} (as defined in Fig.1) and the average input reactive power were used to determine the positive-(*P*-) and *N*-sequence current references. In [6], the currents were regulated by proportional-integral (PI) controllers in *dq*-frame, which had tracking errors due to the 2h current reference components in *dq*-frame and limited bandwidth of the PI controllers. To solve this problem, a dual current control scheme was proposed in [7], where the *P*- and *N*-sequence currents were regulated in the positive synchronous reference frame (PSRF) and negative synchronous frame (NSRF) respectively. However, in this method, the pulsating power in the line impedances (p_R+p_L) was not taken into account. The DC bus voltage depends on the instantaneous output power p_{out} rather than the input power p_{in}, as shown in Fig.1. The power in the line impedances fluctuates when the impedances or the 3-phase currents are unbalanced and thus p_{out} fluctuates even when p_{in} is constant, which will cause DC bus voltage ripple.

The second method is the input-output-power control [9, 10]. Since the 2h DC bus voltage depends on the 2h power in p_{out} rather than p_{in}, the 2h power in p_{out}, the average input active power p_{in}, and the average input reactive power were used to calculate the required *P*- and *N*-sequence current references. Since the 2h power in p_{out} is taken into account, this method is capable of suppressing the 2h power under any unbalanced

operation conditions. To avoid tracking errors in the current regulators [6] and to avoid use of notch filters for the extraction of *P*- and *N*-sequence currents, which can affect bandwidth of the current control loop as shown in [7], the resonant control was employed in [9-12]. In particular, the proportional plus resonant (PR) control in stationary reference frame was employed in [10, 12], and the proportional-integral plus resonant (PI-R) control in the PSRF was employed in [11].

The third method is the output power control [4], where the 2h power in p_{out}, the average power in p_{out}, and average output reactive power were used for the calculation of the *P*- and *N*-sequence current references. This method is also robust to generalized asymmetries as it takes into account the 2h power in p_{out}. Furthermore, this method is simple as it does not require any extraction methods for *P*- sequence and *N*-sequence components of e_a, e_b and e_c in Fig.1.

In the second and third method, the *P*- and *N*-sequence output voltages are essential for the calculation of the *P*- and *N*-sequence current references. For example, the notch filter was employed in [9-11] and the dual second-order generalized integrator (DSOGI) method [15] was employed in [12]. The above methods affect the system dynamic performance and are not easy to tune. This problem was dealt with in [4] and [16] where the *P*- sequence and *N*-sequence output voltages were estimated under the assumption that the line impedances were balanced. However, the *P*- and *N*–sequence decomposers for the currents and supply voltages were still required in [4] and [16]. More specifically, the sequence separation delaying method [17] was employed to extract *P*- and *N*-sequence supply voltages in [4, 16] and the notch filter method [7] was employed to extract *P*- and *N*-sequence currents in [4].

From the aforementioned papers [9-12], the second and third methods can essentially deal with the 2h DC bus voltage regardless of the type of asymmetries. However, the *P*- and *N*-sequence output voltage decomposers are still required, which increase the control complexity. In terms of regulating the *P*- and *N*-sequence currents , the dual current control [7], the proportional and resonant (PR) control in stationary reference frame [10, 12] or the PI-R control in the PSRF [11] can be employed. In the last two methods, the *P*- and *N*-sequence current decomposers can be avoided.

In this paper, a simplified instantaneous power control is proposed to suppress the 2h DC bus voltage under generic unbalance conditions without any sequential component decomposers. Firstly, the proposed method does not require any *P*- and *N*-sequence decomposers to extract the *P*- and *N*-sequence output voltages, which are obtained directly from the outputs of the current PI-R controllers. Secondly, unlike the model-based estimation method [4, 16] to estimate the *P*- and *N*-sequence output voltages, which is sensitive to the parameters, the proposed method is robust to generalized unbalance conditions even when the line impedances are unbalanced. The feasibility of the proposed method is verified on a small-scale three-phase permanent magnet synchronous generator (PMSG) with inherent asymmetry. In addition, the method is tested on the prototype system when different external asymmetries were introduced deliberately in the line impendences.

II. REVIEW OF OUTPUT POWER CONTROL

From Fig.1, it can be deduced that [18]

$$i_c = C\frac{dv_{dc}}{dt} = \frac{p_1 - p_2}{v_{dc}} = \frac{-p_2}{v_{dc}} - \frac{v_{dc}}{R_L} \qquad (1)$$

where v_{dc} is the DC bus voltage, while p_1, p_2 and p_c are the instantaneous powers at the dc side of the system shown in Fig.1. Equation (1) indicates that there will be the 2h voltage in v_{dc} when there is a 2h power component in p_1 or p_2 [2-4].

Assume the power p_2 in unbalanced system with 2h power can be expressed as [19]

$$p_2 = p_2^{dc} + p_2^{2nd} = p_2^{dc} + P_2^{2nd}\cos(2\theta_e + \theta_2) \qquad (2)$$

where θ_e is the electrical rotor position, p_2^{dc} is the average power, P_2^{2nd} and θ_2 are the amplitude and displacement angle of the 2h power.

Assuming the DC bus voltage can be expressed as

$$v_{dc} = v_{dc0} + V_{dc}^{2nd}\cos(2\theta_e + \theta_{2v}) + \dots \qquad (3)$$

where V_{dc}^{2nd} and θ_{2v} are the amplitude and offset angle of the 2h DC bus voltage respectively. Substituting (2) and (3) into (1), the 2h DC bus voltage amplitude can be deduced as

$$V_{dc}^{2nd} = \frac{P_2^{2nd}R_L}{2v_{dc0}\sqrt{1+\left(\omega_e C R_L\right)^2}} \qquad (4)$$

According to (4), the 2h DC bus voltage capacitor is proportional to the amplitude of the 2h power resulted from asymmetries. Although the 2h DC bus voltage can be reduced by increasing capacitance, however, the capacitor size, current and system cost are increased as well. Meanwhile, the 2h DC bus voltage cannot be eliminated in theory in principle.

If the converter is a lossless system, the 2h DC bus voltage will be affected directly by the 2h power in p_{out}. As shown in (4), to eliminate the 2h DC bus voltage, the 2h power should be eliminated.

As detailed in [7], the unbalanced three-phase components without zero sequence components can be expressed as the sum of orthogonal *P*- and *N*-sequence components, i.e.

$$F_{\alpha\beta} = e^{j\theta_e}F_{dq}^p + e^{-j\theta_e}F_{dq}^n \qquad (5)$$

where F can be voltage v or current i. θ_e is the rotor position in machine drive applications or the grid angle in grid applications, and $F_{\alpha\beta}$ can be expressed as

$$F_{\alpha\beta} = F_\alpha + jF_\beta = \frac{2}{3}\left(F_a + F_b \cdot e^{j2\pi/3} + F_c \cdot e^{j4\pi/3}\right) \qquad (6)$$

where F_a, F_b, and F_c are the phase voltages or currents.

In (5), $e^{j\theta_e}F_{dq}^p$ and $e^{-j\theta_e}F_{dq}^n$ are respectively the *P*- and *N*-sequence components in the stationary α-β frame. F_{dq}^p denotes the *P*-sequence components in PSRF, F_{dq}^n denotes *N*-sequence components in the NSRF, and they can be expressed as

$$F_{dq}^p = F_d^p + jF_q^p \qquad (7)$$

$$F_{dq}^n = F_d^n + jF_q^n \qquad (8)$$

where subscripts *d* and *q* denote *d*-axis and *q*-axis components respectively, while superscripts *p* and *n* denote *P*- and *N*-sequence components respectively.

The instantaneous active and reactive powers at the converter three-phase terminals, as shown in Fig.1, can be expressed as [20]

$$p_{out} = \frac{3}{2}\left(v_\alpha i_\alpha + v_\beta i_\beta\right) \tag{9}$$

$$q_{out} = \frac{3}{2}\left(v_\alpha i_\beta - v_\beta i_\alpha\right) \tag{10}$$

By substituting v_α, v_β, i_α and i_β in (9) and (10) by that in (5), the instantaneous active and reactive powers can be deduced as [4, 7]

$$p_{out} = p_{out0} + p_{out\_c2}\cos(2\theta_e) + p_{out\_s2}\sin(2\theta_e) \tag{11}$$

$$q_{out} = q_{out0} + q_{out\_c2}\cos(2\theta_e) + q_{out\_s2}\sin(2\theta_e) \tag{12}$$

where p_{out0} is the average active power in p_{out}, q_{out0} is the average reactive power in q_{out} while p_{out_c2}, p_{out_s2}, q_{out_c2} and q_{out_s2} are the coefficients of the 2h active and reactive power components which are given by:

$$\begin{bmatrix} p_{out0} \\ q_{out0} \\ p_{out\_c2} \\ p_{out\_s2} \end{bmatrix} = \frac{3}{2} \begin{bmatrix} v_d^p & v_q^p & v_d^n & v_q^n \\ -v_q^p & v_d^p & -v_q^n & v_d^n \\ v_d^n & v_q^n & v_d^p & v_q^p \\ v_q^n & -v_d^n & -v_q^p & v_d^p \end{bmatrix} \begin{bmatrix} i_d^p \\ i_q^p \\ i_d^n \\ i_q^n \end{bmatrix} \tag{13}$$

If p_{out_c2} and p_{out_s2} in (13) are set at zero and p_{out0} and q_{out0} are respectively set to be equal to their reference values $p_{out0}{}^*$ and $q_{out0}{}^*$, the P- and N-sequence current references can be obtained from (13) as

$$\begin{bmatrix} i_d^{p*} \\ i_q^{p*} \\ i_d^{n*} \\ i_q^{n*} \end{bmatrix} = \frac{2p_{out0}^*}{3D_1} \begin{bmatrix} v_d^p \\ v_q^p \\ -v_d^n \\ -v_q^n \end{bmatrix} + \frac{2q_{out0}^*}{3D_2} \begin{bmatrix} -v_q^p \\ v_d^p \\ -v_q^n \\ v_d^n \end{bmatrix} \tag{14}$$

where superscript "*" denotes reference values and D_1 and D_2 can be expressed as (15) and (16) respectively.

$$D_1 = \left(v_d^p\right)^2 + \left(v_q^p\right)^2 - \left(v_d^n\right)^2 - \left(v_q^n\right)^2 \tag{15}$$

$$D_2 = \left(v_d^p\right)^2 + \left(v_q^p\right)^2 + \left(v_d^n\right)^2 + \left(v_q^n\right)^2 \tag{16}$$

If the current controllers can trace the current references (14) without tracking errors, p_{out_c2} and p_{out_s2} in (13) will be zero. Consequently, the 2h active power components in (11) will be also zero. Therefore, the 2h DC bus voltage can be suppressed according to (1).

III. PROPOSED CONTROL STRATEGY

As shown in (14), the P- and N-sequence output voltages are essential for the calculation of P- and N-sequence current references that are used in the instantaneous output power control to eliminate the 2h power in p_{out}. In this section, a prototype asymmetric PMSG will be employed to demonstrate the principles of extraction of P- and N-sequence output voltages in an unbalanced three-phase system. Firstly, the extraction of P- and N-sequence voltages with the aid of PI-R controllers in PSRF will be introduced, and then the scheme of the proposed instantaneous power control will be presented.
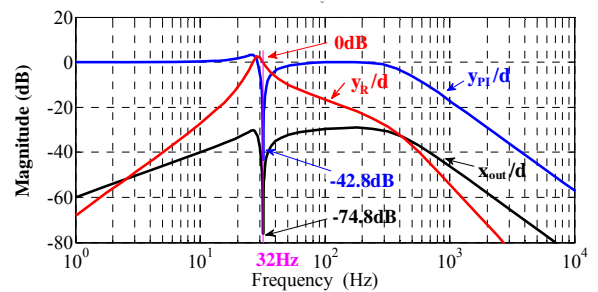
A) Extraction of the P- and N-Sequence Output Voltages
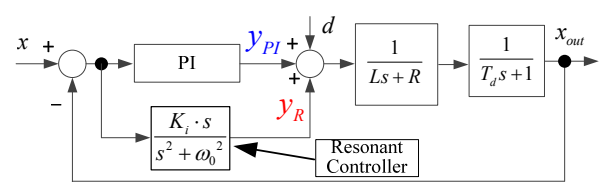
(a) Equivalent transfer function
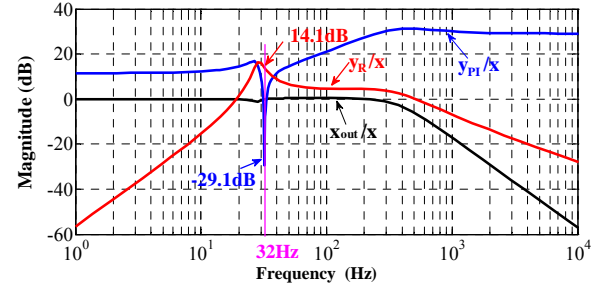
(b) Bode magnitude (input)

(c) Bode magnitude (disturbance)

Fig.2 Proposed extraction of P- and N-sequence output voltages.

In general, an asymmetric PMSG in dq-frame can be represented by a linear resistance-inductance (RL) model with a 2h disturbance component [21, 22] and this modeling approach is used in this work. The block diagram of the proposed current control loop with the PI-R controller in the PSRF is shown in Fig.2(a), where T_d is the total delay time that includes delays due to both current sampling and PWM. In Fig.2(a), x and x_{out} denote the current reference and the current feedback in dq-frame respectively, while y is the output voltage in dq-frame and d is the 2h voltage disturbance.

The integral term in the resonant controller is approximated by an equivalent low-pass filter as in [20] and [21].The transfer function of the resonant controller can then be simplified as

$$R(\omega_0) = \frac{2K_i\omega_c s}{s^2 + 2\omega_c s + \omega_0} \tag{17}$$

where ω_c is the cut-off frequency of the low-pass filter, ω_0 is the resonant frequency and is much higher than ω_c, while K_i is the integral gain. In this case study, a low-pass filter with the cut-off frequency of $\omega_c = \omega_0/1000$ was employed and the integral gain of the resonant controller is set to be the same as the integral gain of the PI controller. The proportional gain K_p and the integral gain K_i of the PI controller are optimized based on the pole-zero cancellation principle [23]. In particular, $K_p = L/(2T_d)$ and $K_i = R/(2T_d)$ with damping factor of 0.707, where R, L and T_d are equal to 3.76Ω, 17mH and 300μs respectively.

The results shown in Fig.2(b) and Fig.2(c) were obtained for the prototype PMSG when operated at a frequency of 16Hz with a resonant frequency of the PI-R controller set at 32Hz. From the Bode magnitude plots of x_{out}/x, y_{PI}/x and y_R/x in Fig.2(b), it can be seen that the 2h voltage (32Hz) in y_R is dominant while that in y_{PI} is negligible if there is a 2h component in current reference x. Meanwhile, the dc component of the output voltage in y_{PI} is dominant while that in y_R is negligible, which means that the dc and 2h component in the output voltage can be separated.

The Bode magnitude plots of x_{out}/d, y_{PI}/d and y_R/d are shown in Fig.2 (c). If there is a 2h component in d, it can be seen that the 2h current in x_{out} is suppressed effectively. Meanwhile, the 2h voltage in y_R is almost equal to d while that in y_{PI} is negligible. If there is a dc component in the disturbance d, the DC component in y_{PI} will be equal to the dc component in d as the magnitude of y_{PI}/d at the zero frequency is 0dB, while the dc component in y_R is negligible.

Overall, the dc and 2h components of the output voltage in the PSRF can be separated effectively by the PI plus resonant controller when there is a 2h component in the current reference or there is a dc and 2h component in the disturbances. Therefore, the outputs of the *PI* plus resonant controller can be employed directly to represent the dc and 2h components of the output voltage.

B) Proposed Method

The detailed control block diagram of the proposed instantaneous power control is shown in Fig.3. The current reference calculation is shown in Fig.3(a), which is obtained according to (14). The average output reactive power reference is assigned to zero for the unity power factor. $T_{dq}(\theta)$ is the standard Park transformation (18). Using matrix $T_{dq}(2\theta_e)$, the N-sequence current references in the NSRF (i.e. dc values) are converted to the ac values ($2\omega_e$) in PSRF. Therefore, there are dc values and ac values at a frequency of $2\omega_e$ in the current references in PSRF.

$$T_{dq}(\theta) = \begin{bmatrix} \cos(\theta) & \sin(\theta) \\ -\sin(\theta) & \cos(\theta) \end{bmatrix} \quad (18)$$

The current control scheme is shown in Fig.3(b). By employing a PI-R controller at a resonant frequency of $2\omega_e$ in the PSRF [11], the currents can be regulated effectively in the PSRF without tracking errors.

As shown in Fig.3(b), the P-sequence voltages in PSRF are directly obtained from the output of the PI controllers, while the N-sequence voltages in the PSRF are directly obtained from the output of the resonant controllers in the PSRF due to its high gain at the resonant frequency of $2\omega_e$. Using matrix conversion $T_{dq}(-2\theta_e)$, the N-sequence voltages ($2\omega_e$) in the PSRF are converted to the DC components in the NSRF. Therefore, the N-sequence output voltages in the NSRF can be obtained easily. Then the currents can be obtained by (14) if the actual output voltage is equal to the voltage reference. Since the P- and N-sequence output voltages are from PI-R controller without any information of asymmetries, they are robust to any asymmetry in the system.
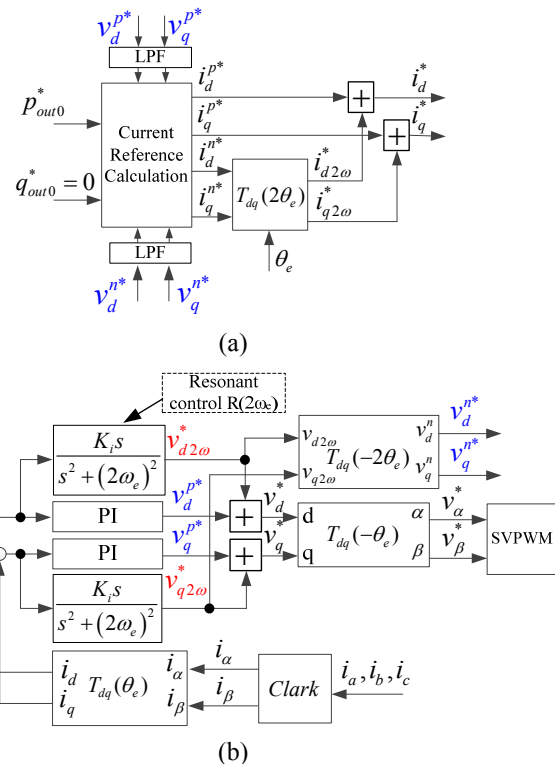

(a)

(b)

Fig.3 Proposed instantaneous power control for suppressing the 2h DC bus voltage. (a) Current reference generation. (b) Current control scheme.

IV. EXPERIMENTS

A small-scaled asymmetric three-phase prototype PMSG system is employed to verify the proposed instantaneous power control for unbalanced three-phase systems. The winding topology of the PMSG is asymmetric that results in the inherent asymmetry with the unbalanced inductances. The no-load inductances measured by HIOKI LCR meter IM3533-01 at the frequency of 120Hz and the fitting-curves are shown in Fig.4. It is apparent that the average mutual inductance M_{AB} is different with respect to the mutual inductances M_{AC} and M_{BC}, which indicates that the PMSG is unbalanced.

The test rig is illustrated in Fig.5, a servo machine is coupled with the PMSG, which is used to simulate the wind turbine. A power resistor R_L of nominal $100\,\Omega$ is connected to the DC bus to consume the power generated by the PMSG. The DC bus capacitor of 1500μF is employed. The experiments are based on dSPACE DS1006 and the calculation rate of the current loop is configured to be 5 kHz, which is the same as the PWM frequency.

In this section, the balanced current control will be firstly investigated. As expected, the 2h power and DC bus voltage will be produced due to the above explained inherent asymmetries of the PMSG. Then the proposed instantaneous power control will be employed. It will be demonstrated that the 2h component in DC bus power and voltage can be suppressed effectively. Hereafter, the extraction of the P- and N-sequence output voltages in the experiments will be analyzed in detail. Finally, it will be verified that the proposed method is applicable under different asymmetries.
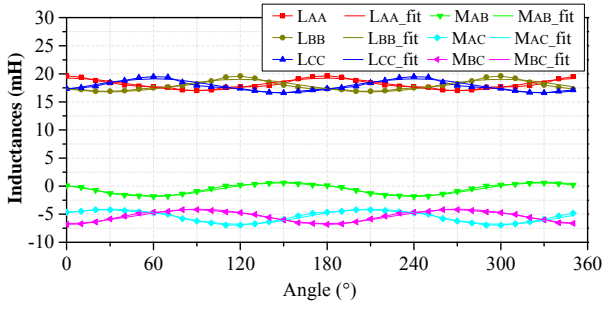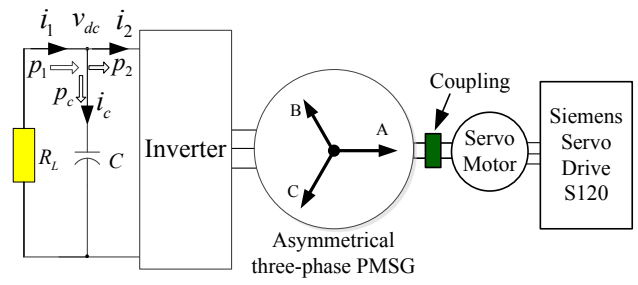
Fig.4 Measured inductances.
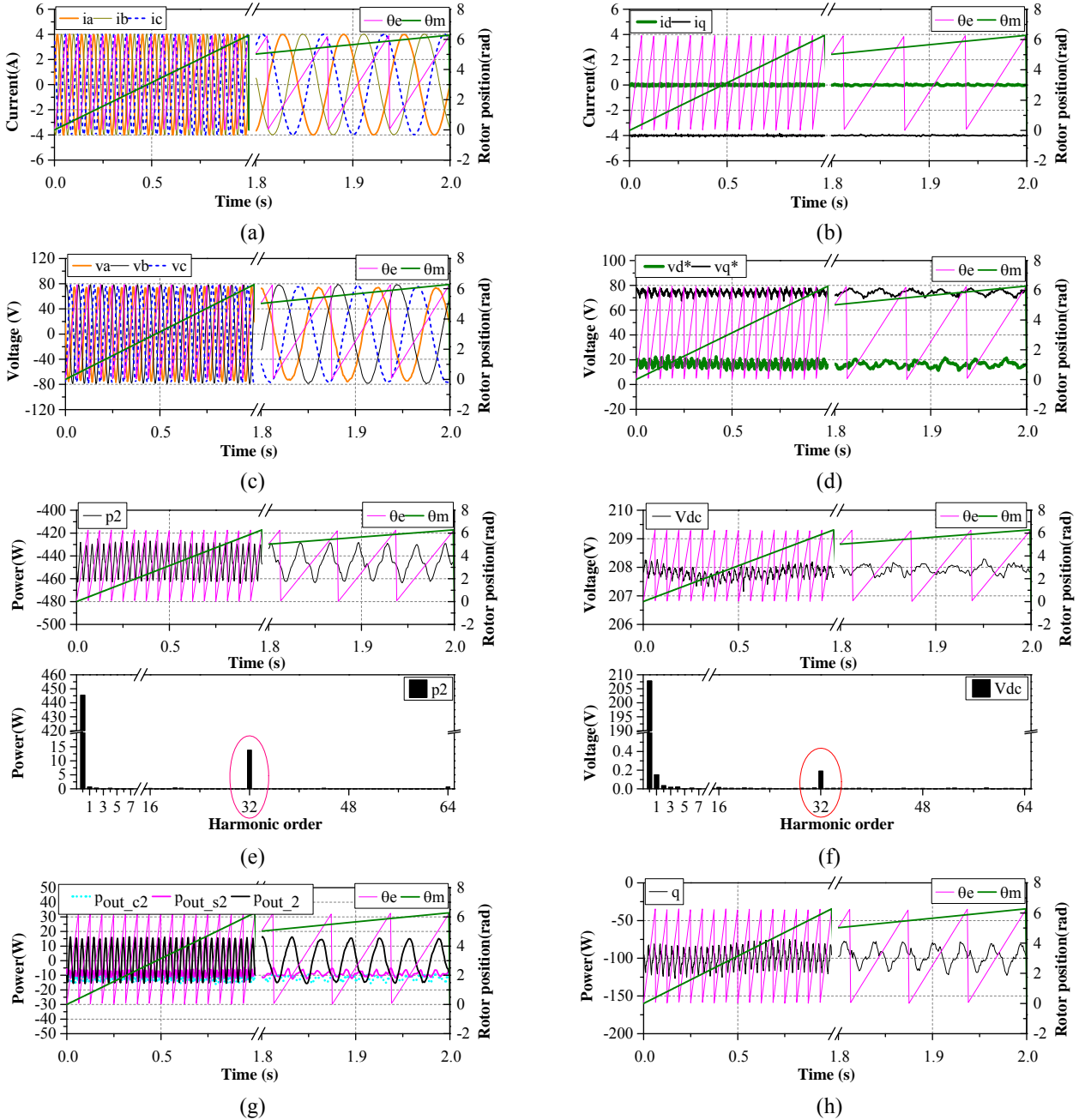

Fig.5 Illustration of the test rig.

(a)

(b)

(c)

(d)

(e)

(f)

(g)

(h)

Fig.6 Balanced current control, harmonic analysis based on mechanical frequency. (a) Phase currents. (b) dq-axis currents. (c) Phase voltages. (d) dq-axis voltages. (e) Active power and harmonic analysis. (f) DC bus voltage and harmonic analysis. (g) 2h active power coefficients and 2h active power. (h) Reactive power.
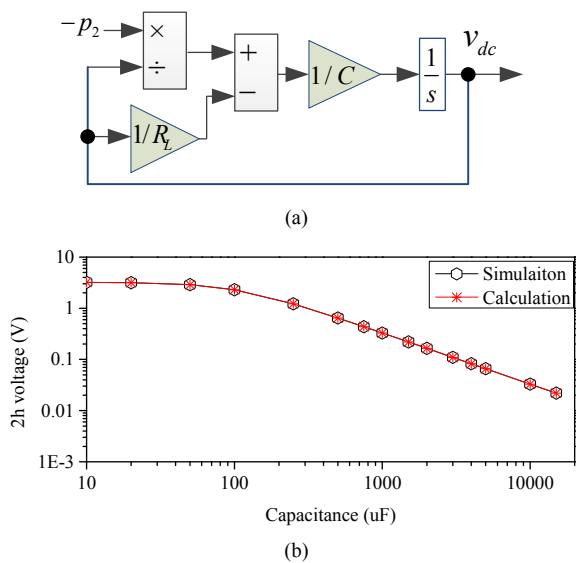
(a)

(b)

Fig.7 Second harmonic DC voltage with respect to different capacitance. (a) Simplified simulation flowchart. (b) 2h DC bus voltage vs. capacitance

(1) Balanced Current Control

In this experiment, the d-axis and q-axis current references in the PSRF in Fig.3(a) are set to 0A and -4A respectively, while the N-sequence current references in the NSRF are zero. Therefore, the instantaneous power control is excluded. The speed is regulated to be 60rpm by the servo motor. Since the q-axis current is negative, the PMSG works in generation mode.

The experimental results are shown in Fig.6. As can be seen from Fig.6(b), the dq-currents are fairly regulated. Therefore, the phase currents are very balanced Fig.6(a). However, due to the unbalanced impedances of the asymmetric PMSG, the output phase voltages are unbalanced, which is indicated by the different amplitudes of the phase voltages, Fig.6(c) and the 2h components in dq-axis voltages Fig.6(d). The 2h active power coefficients in (13) are shown in Fig.6(g), they are approximately 10W, therefore, the 2h power designated as p_{out2} in (11) can be obtained and shown in Fig.6(g), which shows that there is apparent 2h power in the active power. Consequently, the instantaneous active power p_2 (equal to p_{out} neglecting the inverter losses) has apparent oscillations as shown in Fig.6(e). The harmonic analysis of the active power is shown in Fig. 6(e) and it is based on the mechanical frequency of the PMSG which has 16 pole pairs. It is apparent that the 2h component in the active power is dominant. Therefore, the 2h DC bus voltage ripple, Fig.6(f), is obvious. Meanwhile, as shown in Fig. 6(h), the average reactive power is -100W. Similar to the active power in Fig. 6(e), there is also apparent 2h component in reactive power in Fig. 6(h).

It is noting that the capacitance has significant impact on the DC bus voltage oscillation(4). To investigate the relationship of 2h DC bus voltage with respect to the 2h power, the simplified simulation based on Fig.1 can be shown in Fig.7(a). Based on the results in this experiment (average power -445.4W, 2h power 13.79W, operating frequency 16Hz, R_L 97Ω), the 2h DC bus voltage with respect to different capacitances from simulation Fig.7(a) and from calculation (4)

can be shown in Fig.7(b). It shows that the 2h DC bus voltage decreases as the capacitance increases. To guarantee the 2h DC bus voltage is smaller than 0.1V, the capacitance has to be larger than 3000μF in this case. Nevertheless, the 2h DC bus voltage still cannot be eliminated even the capacitance is larger than 10000 μF.

(2) Proposed Instantaneous Power Control

The experimental results of the proposed method are shown in Fig.8. In this experiment, the speed is regulated to be 60rpm by the servo motor. The average active and reactive power references for the PMSG in Fig.3(a) are assigned to -400W and 0W respectively and the PMSG works in generation mode. From the active power and the corresponding harmonic analysis, Fig.8(e), it can be seen that the average active power is -400W, which means that the active power is fairly regulated. From the reactive power in Fig.8(h), it can be seen that the average reactive power is 0W, which means that the average reactive power is fairly regulated as well.

The P-sequence output voltages in the PSRF and N-sequence output voltages in the NSRF are shown in Fig.8 (i), where the DC signals are dominant. The P-sequence current references in the PSRF and N-sequence current references in the NSRF are shown in Fig.8(j). It can be seen that they are DC signals. Since the N-sequence currents in NSRF are not zero, the 2h currents in the dq-axis currents in the PSRF are apparent, Fig.8(b). Therefore, the phase currents shown in Fig.8(a) are more unbalanced than those in Fig.6(a). Due to the unbalanced currents and the unbalanced impedances, the output voltages are unbalanced as well. As shown in Fig.8(c), the amplitudes of the phase voltages are different. Consequently, there are apparent 2h voltages in the dq-axis voltages in PSRF, Fig.8(d).

As the N-sequence currents are injected into the stator currents to suppress the 2h active power, the 2h active power coefficients in (13) are almost zero in Fig.8(g). Therefore, as can be seen from Fig.8(e), the 2h active power is much smaller than that in Fig.6(e). Consequently, the 2h DC bus voltage in Fig.8(f) is much smaller than that in Fig.6(f).

It is worth noting that although the average reactive power is zero, Fig.8(j), the 2h reactive power is evident since the coefficients of the 2h reactive power in (12) are not involved in the calculations of the current references(14).

(3) Extraction of P- and N-sequence Output Voltages

The extraction of the P- and N-sequence output voltages in the balanced current control and the proposed method with the aid of PI-R control are shown in Fig.9. It can be seen from Fig.9(a) that the dominant DC values are in the outputs of the PI controllers (i.e., $V_{dp}*$ and $V_{qp}*$) rather than in the outputs of the resonant controllers (i.e. $V_{d2\omega}*$ and $V_{q2\omega}*$), which means that almost all the P-sequence voltages are mapped to $V_{dp}*$ and $V_{qp}*$. It can be also seen from Fig.9(b) that the dominant 2h output voltages are in $V_{d2\omega}*$ and $V_{q2\omega}*$ rather than in $V_{dp}*$ and $V_{qp}*$, which means that nearly the entire 2h output voltages are mapped to $V_{d2\omega}*$ and $V_{q2\omega}*$. Therefore, the P- and N-sequence voltages can be separated effectively by the PI-R control, which means that the specific sequence component decomposers such as the time delaying method, the notch filter method, or the DSOGI method, are not necessarily required.
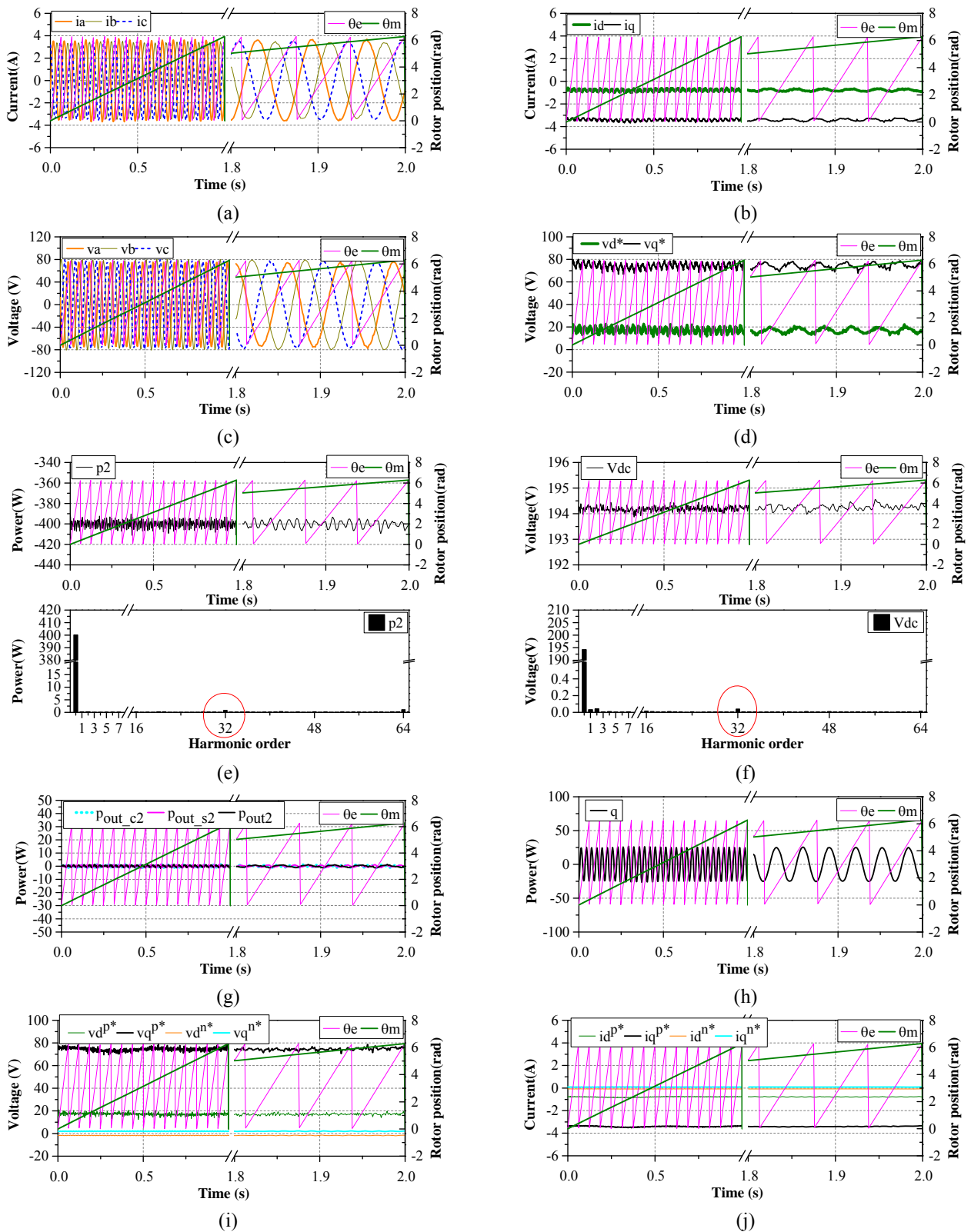
Fig.8 Experimental results of proposed method. (a) Phase currents. (b) *dq*-axis currents. (c) Phase voltages. (d) *dq*-axis voltages. (e) Active power and harmonic analysis. (f) DC bus voltage and harmonic analysis. (g). 2h active power coefficients and 2h active power. (h) Reactive power. (i) *P*-sequence voltages in PSRF and *N*-sequence voltages in NSRF. (j) *P*-sequence currents in PSRF and *N*-sequence currents in NSRF.
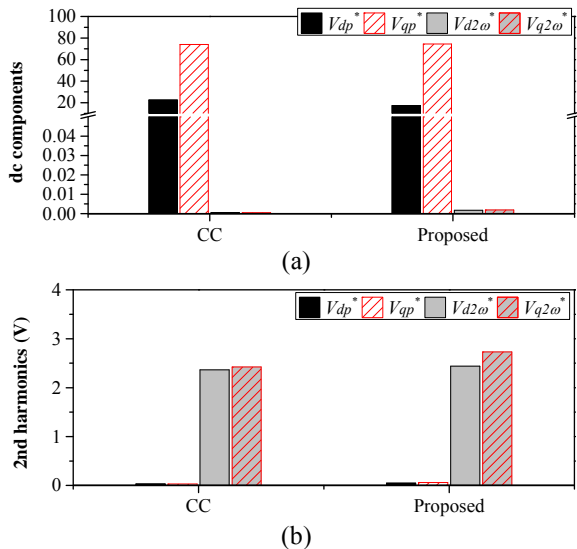
Fig.9 Extraction of the *P*- and *N*-sequence voltages (CC: balanced current control, Proposed: proposed power control). (a) DC components. (b) Second harmonics.

(4) Different Asymmetries

In the following experiments, an external inductor is deliberately connected in series with phases *A*, *B*, and *C* respectively. The equivalent inductance and resistance of the inductor are 5.63mH and 1.15Ω respectively. The inherent and extra asymmetries are summarized in TABLE I.

The experimental results with different DC bus capacitors (3000μF or 1500μF) and different asymmetries are shown in Fig.10, where "inherent" denotes the inherent asymmetry, "phase A", "phase B", and "phase C" mean the corresponding phase is connected deliberately with the external inductor in series, the "CC" means constant current control, the "Proposed" means the proposed power control. The capacitance in Fig.10 means the DC bus capacitance of DC bus capacitor is 3000μF or 1500μF when the experiments are conducted. The experimental results show that the 2h power and DC bus voltage can be effectively suppressed by the proposed method under different asymmetric conditions.

V. CONCLUSION

A simplified instantaneous power control of suppressing the 2h DC bus voltage without *P*- and *N*-sequence component decomposers under generic unbalanced conditions has been proposed in this paper. No specific *P*- and *N*-sequence component decomposers, such as the time delaying method, notch filter method, or DSOGI method, are required for the extraction of *P*- and *N*-sequence currents and output voltages. Since the proposed method does not require any information of the asymmetry, it is robust to different types of asymmetries. The capability of suppressing the 2h power and DC bus voltage has been verified on an asymmetric three-phase prototype PMSG system with considerable inherent asymmetries and deliberately introduced asymmetries.

TABLE I
ASYMMETRIES IN DIFFERENT CASES

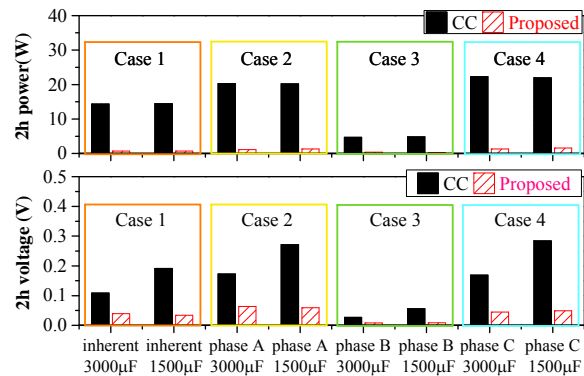| Cases	Asymmetries
Case 1	Inherent asymmetry
Case 2	Extra asymmetry @ external inductor in phase *A*
Case 3	Extra asymmetry @ external inductor in phase *B*
Case 4	Extra asymmetry @ external inductor in phase *C*

Fig.10 Comparison of the 2h power and DC bus voltage under the conditions of different asymmetries and DC link capacitors.

REFERENCE

[1] R. Reginatto and R. A. Ramos, "On electrical power evaluation in dq coordinates under sinusoidal unbalanced conditions," *IET Generation, Transmission & Distribution,* vol. 8, no. 5, pp. 976-982, 2014.

[2] L. Xiao, S. Huang, and K. Lu, "DC-bus voltage control of grid-connected voltage source converter by using space vector modulated direct power control under unbalanced network conditions," *IET Power Electron.,* vol. 6, no. 5, pp. 925-934, 2013.

[3] J. Tan, X. Wang, Z. Chen, and M. Li, "Impact of a direct-drive permanent magnet generator (DDPMG) wind turbine system on power system oscillations," in *Proc. IEEE Power and Energy Soc. General Meeting*, 2012, pp. 1-8.

[4] Y. Bo, R. Oruganti, S. K. Panda, and A. K. S. Bhat, "An output-power-control strategy for a three-phase PWM rectifier under unbalanced supply conditions," *IEEE Trans. Ind. Electron.,* vol. 55, no. 5, pp. 2140-2151, 2008.

[5] K. Lee, T. M. Jahns, G. Venkataramanan, and W. E. Berkopec, "DC-bus electrolytic capacitor stress in adjustable-speed drives under input voltage unbalance and sag conditions," *IEEE Trans. Ind. Appl.,* vol. 43, no. 2, pp. 495-504, 2007.

[6] P. Rioual, H. Pouliquen, and J.-P. Louis, "Regulation of a PWM rectifier in the unbalanced network state using a generalized model," *IEEE Trans. Power Electron.,* vol. 11, no. 3, pp. 495-502, 1996.

[7] S. Hong-Seok and N. Kwanghee, "Dual current control scheme for PWM converter under unbalanced input voltage conditions," *IEEE Trans. Ind. Electron.,* vol. 46, no. 5, pp. 953-959, 1999.

[8] J. G. Hwang, P. W. Lehn, and M. Winkelnkemper, "Control of grid connected AC-DC converters with minimized DC link capacitance under unbalanced grid voltage condition," in *Proc. European Conf. Power Electron. and Appl.*, 2007, pp. 1-10.

[9] S. Yongsug and T. A. Lipo, "Control scheme in hybrid synchronous stationary frame for PWM AC/DC converter under generalized unbalanced operating conditions," *IEEE Trans. Ind. Appl.,* vol. 42, no. 3, pp. 825-835, 2006.

[10] J. Hu and Y. He, "Modeling and control of grid-connected voltage-sourced converters under generalized unbalanced operation conditions," *IEEE Trans. Energy Convers.,* vol. 23, no. 3, pp. 903-913, 2008.

[11] J. B. Hu, Y. K. He, L. Xu, and B. W. Williams, "Improved control of DFIG systems during network unbalance using PI-R current regulators," *IEEE Trans. Ind. Electron.,* vol. 56, no. 2, pp. 439-451, 2009.

[12] D. Roiu, R. I. Bojoi, L. R. Limongi, and A. Tenconi, "New stationary frame control scheme for three-phase PWM rectifiers under unbalanced

voltage dips conditions," *IEEE Trans. Ind. Appl.,* vol. 46, no. 1, pp. 268-277, 2010.

[13] A. Yazdani and R. Iravani, "A unified dynamic model and control for the voltage-sourced converter under unbalanced grid conditions," *IEEE Trans. Power Del.,* vol. 21, no. 3, pp. 1620-1629, 2006.

[14] X. H. Wu, S. K. Panda, and J. X. Xu, "Analysis of the instantaneous power flow for three-phase PWM boost rectifier under unbalanced supply voltage conditions," *IEEE Trans. Power Electron.,* vol. 23, no. 4, pp. 1679-1691, 2008.

[15] P. Rodriguez, R. Teodorescu, I. Candela, A. V. Timbus, M. Liserre, and F. Blaabjerg, "New positive-sequence voltage detector for grid synchronization of power converters under faulty grid conditions," in *Proc. 37th IEEE Power Electron. Spec. Conf.*, 2006, pp. 1-7.

[16] Z. Li, Y. Li, P. Wang, H. Zhu, C. Liu, and W. Xu, "Control of three-phase boost-type PWM rectifier in stationary frame under unbalanced input voltage," *IEEE Trans. Power Electron.,* vol. 25, no. 10, pp. 2521-2530, 2010.

[17] S. Yongsug, V. Tijeras, and T. A. Lipo, "A nonlinear control of the instantaneous power in dq synchronous frame for PWM AC/DC converter under generalized unbalanced operating conditions," in *Proc. Conf. Record of the 37th IAS Annu. Meeting Ind. Appl. Conf.*, 2002, pp. 1189-1196 vol.2.

[18] Y. Ye, M. Kazerani, and V. H. Quintana, "A novel modeling and control method for three-phase PWM converters," in *Proc. IEEE 32nd Annual Power Electronics Specialists Conference (PESC)*, 2001, pp. 102-107 vol. 1.

[19] K. Hyosung, F. Blaabjerg, B. Bak-Jensen, and C. Jaeho, "Instantaneous power compensation in three-phase systems by using p-q-r theory," *IEEE Trans. Power Electron.,* vol. 17, no. 5, pp. 701-710, 2002.

[20] H. Akagi, Y. Kanazawa, and A. Nabae, "Instantaneous reactive power compensators comprising switching devices without energy storage components," *IEEE Trans. Ind. Appl.,* vol. IA-20, no. 3, pp. 625-630, 1984.

[21] C. B. Jacobina, M. B. d. Correa, T. M. Oliveiro, A. M. N. Lima, and E. R. Cabral da Silva, "Current control of unbalanced electrical systems," *IEEE Trans. Ind. Electron.,* vol. 48, no. 3, pp. 517-525, 2001.

[22] H. S. Kim, H. S. Mok, G. H. Choe, D. S. Hyun, and S. Y. Choe, "Design of current controller for 3-phase PWM converter with unbalanced input voltage," in *Proc. 29th Annual IEEE Power Electronics Specialists Conference*, 1998, pp. 503-509 vol.1.

[23] V. Blasko, V. Kaura, and W. Niewiadomski, "Sampling of discontinuous voltage and current signals in electrical drives: a system approach," *IEEE Trans. Ind. Appl.,* vol. 34, no. 5, pp. 1123-1130, 1998.

Yashan Hu received the B.Eng. and M.Sc. degrees in Electronic and Electrical Engineering from the Northwestern Polytechnical University, Xi'an, China, in 2002 and 2005, respectively. He has been working toward the Ph.D. degree at the University of Sheffield, Sheffield, U.K., since Jun 2012.

From 2005 to 2012, he was with Delta Green Tech (China) Co., Ltd., Shanghai, China, Shanghai Yungtay Elevator Co. Ltd as a Research Engineer, and Shanghai Welling Motor R&D Centre as Project Manager. His research interests are control of electric drives.

Z. Q. Zhu (M'90–SM'00–F'09) received the B.Eng. and M.Sc. degrees from Zhejiang University, Hangzhou, China, in 1982 and 1984, respectively, and the Ph.D. degree from the University of Sheffield, Sheffield, U.K., in 1991, all in electrical engineering.

From 1984 to 1988, he lectured in the Department of Electrical Engineering, Zhejiang University. Since 1988, he has been with the University of Sheffield, where since 2000, he has been a Professor of electrical machines and control systems in the Department of Electronic and Electrical Engineering, and is currently the Head of the Electrical Machines and Drives Research Group. His current major research interests include the design and control of permanent-magnet brushless machines and drives for applications ranging from automotive to renewable energy.

Milijana Odavic (M'13) received the M.Sc. degree in electrical and electronic engineering from the University of Zagreb, Zagreb, Croatia, in 2004 and the Ph.D. degree from the University of Nottingham, Nottingham, U.K., in 2008.

In 2013, she became a Lecturer in Power Electronics in the Department of Electronic and Electrical Engineering at the University of Sheffield, Sheffield, U.K. Prior to joining the University of Sheffield, she was a Research Fellow in the Power Electronics, Machines and Control Group at the University of Nottingham and in the Department of Electric Machines, Drives and Automation at the University of Zagreb. Her current research interests include modelling and control of power electronics dominated micro-grids, modelling of real system uncertainty and robust stability, design and control of power electronic converters for enhanced power quality.